Lewis River Case Study Final Report

A decision-support tool for assessing watershed-scale habitat recovery strategies for ESA-listed salmonids

Appendix F: Sediment Routing

May 2007

Introduction

The sediment routing model is used to route sediment delivered to each channel segment from the lateral hillslopes and upstream segments. The lateral and upstream sediment influx is cumulatively routed through each segment to the next downstream segment. The routed sediment estimates are output as habitat metrics and also used as inputs for evaluation models such as the sediment survival model (Appendix K).

Our goals are to identify the sources and transport pathways for sediment entering the river system. Ideally, we would also determine corresponding transport rates and sediment transit times, with associated channel morphologies, bed textures, and stability, for all points in the channel system.

The first goal is approachable: basin topography, together with geologic, soil type, and land-cover mapping, can be used to identify source locations and estimate sediment input rates to channels. Topography can also be used to delineate the channel network and determine flow paths for all points in the basin. The second goal is less approachable: controls on sediment transport are numerous and complex, far beyond our data sources to characterize completely. Nevertheless, we can generalize.

Using gross morphologic indicators of drainage area, channel gradient, and valley width, we can broadly delineate different channel types and identify potential zones of transport and deposition (e.g., Montgomery and Buffington 1997). When coupled with basin-specific empirical data, such generalizations can be used to predict channel conditions and responses to changes upstream.

Here, we describe the processes of sediment routing for the Lewis River basin. Many steps entail GIS exercises to relate disparate data sources and to extract needed information for the actual sediment routing. All GIS programming tasks were done in FORTRAN95. Microsoft Excel was used for plotting graphs and estimating functional relationships between variables.

Link Segments

The channel network is represented as a series of channel reaches, each reach is represented in a GIS database as a unique geo-referenced arc (referred to here as a segment, in reference to the SHIAPP (2004) terminology), and each segment has associated data that describe attributes of the reach. The SHIAPP segment data shapefile provided information concerning segment locations and attributes, but lacked information indicating how the segments are connected spatially, such as which segments were connected and the direction of flow between them.

All segments are identified with a unique integer value (ID) and segment topology is defined in terms of the up- and downstream segment IDs. In most cases, there is only one upstream segment and one downstream segment; although there are multiple upstream segments at channel confluences and multiple downstream segments where anastomosing channels diverge. Two steps were used to identify the up- and down-stream segments:

1) *Use segment-endpoint locations to identify contiguous segments*.
   Adjacent segment endpoints are coincident. I compared endpoints of all segments to find those that matched. There were no matches for ten reaches. Some of these were completely isolated from the channel network, others crossed another segment, but the endpoints did not match. I visually matched all but two of these.
2) *Use flow direction to determine the up and downstream segments.* Flow directions were determined with the program bld_grds (Miller 2002, 2003), part of the NetStream program set, which constructs a raster file specifying flow direction at each pixel, with pixels defined by the 10-m DEM.

These steps were done using short programs written in FORTRAN95. Up- and down-stream segment ID for each segment is stored in a binary data file, which can be written to an ASCII output file if required.

Delineate Contributing Areas

Sediment inputs from surface erosion, road erosion, and mass wasting are estimated per unit area as functions of surface gradient (and curvature for mass wasting), soil type, land use, forest cover, and road density. These models were developed separately and are described in Appendix E. Estimates of mean annual sediment influx to a segment, excluding inputs from upstream, are calculated for the unique contributing area to the segment, based on its gradients, soil types, land uses, forest cover, and road density. The contributing areas form closed polygons adjacent to the segment, typically one on each side, and are referred to here as “drainage wings.”

Drainage wings were delineated using the flow direction estimated for each DEM pixel. Using a new raster file with pixel values initialized to zero, pixels containing channel segments were flagged with the segment ID. All non-channel pixels were then given the ID of the segment they flow into. Drainage wings are thus delineated at a resolution of 100 m^2, the surface area of a 10-m DEM pixel. The resulting raster file was later used to define a polygon coverage of drainage wings to use for sediment and runoff modeling (Appendix E).

Using this algorithm, drainage wings for some very short segments were not delineated. These segments then have no unique contributing area, but still serve as conduits for water and sediment delivered from upstream. Although a small proportion of the segments ended up with no drainage wings, those that were delineated account for all surface area of the basin.

Cumulative routing of sediment inputs

Output from the erosion models is provided in a row-column format, ASCII data file that gives mean annual sediment inputs (kg) from each drainage wing. Sediment inputs for three sources are reported: surface erosion, mass wasting, and roads (including both surface erosion and mass wasting associated with roads). We further divided sediment inputs into six size classes (Table F-1).

Table F-1. Sediment size classes

Size Class	Size range (mm)	Description
1	<0.25	Fine sand, assumed to be transported as wash load
2	0.25-0.5	Medium sand
3	0.5-1.0	Coarse sand
4	1.0-4.8	Very coarse sand to fine gravel
5	4.8-78	Medium-coarse gravel
6	>78	Cobble

These inputs are summed cumulatively downstream through the channel network, so that the total upstream mean-annual sediment yield can be estimated for each of the sources and for each of the size classes. This information provides an estimate of mean annual sediment yield (in kg) from all upstream sources to each segment (with zero transport assumed through reservoirs).

Downstream fluvial transport results in abrasion of sediment clasts. Because much of the abraded material is small enough to be carried as wash load, bed load volume is systematically reduced with downstream travel. Estimates of mean annual wash load and bed load must therefore account both for inputs to the channel and for changes in volume (reductions to bed load, increases to wash load) associated with abrasion.

Volume loss to abrasion is difficult, perhaps impossible, to measure directly in a river, so tumbling-mill experiments are used to estimate abrasion rates. Volume loss of coarse grains is found to be proportional to the distance traveled:

$$dV = -\beta V dx \quad (1)$$

where V is volume of bed-load-sized material in the mill and x is distance traveled (product of mill circumference, rotations per unit time, and time the mill is run).

Abrasion causes both a loss of total bed load volume and a change in grain-size distribution.

For a given size class, some sediment clasts are lost to the next lower size class, as their size is reduced by abrasion, and some clasts are gained from the next larger size class. The change in volume *v* in a single size class during mill transport is estimated as (Parker 1991):

$$\frac{dv}{dx} = \frac{1}{3}\frac{\partial(v\beta)}{\partial \ln(D)} - v\beta \quad (2)$$

where ln(D) is the natural logarithm of the mean diameter of clasts in the size class. (Clast size is commonly characterized using a log scale, because of the typical abundance of small clasts). If we assume that abrasion in the mill can be used to approximate abrasion during fluvial transport, this equation can be integrated over travel distance x for all size classes to estimate both the change in the grain-size distribution and the loss of bed-load volume to wash load.

The rate of volume loss, specified by β, varies with rock type and abrasion process (Mikos 1995) and is estimated from repeated sieving of material after increments of tumbling using either total volume loss (Eqn. 1, assuming that β is independent of clast size), or from the evolution of the grain-size distribution (Eqn. 2). Tumbling-mill data (Figure F-1) from Tilton River sediment were used (unpublished data, Earth Systems Institute). The Tilton is a tributary of the Cowlitz River to the north of the Lewis River Basin. Both the Tilton and Lewis river basins are underlain by similar volcanic rock types. Using Equation 1, we obtain a value for β of 0.034 km^{-1}, i.e., a volume loss of 3.4% per kilometer of transport.

To apply Equation 2 to estimate changes in grain-size distribution associated with abrasion requires a finely subdivided set of size classes. Sediment volumes in the six size classes specified above were subdivided into smaller logarithmically distributed classes using the following procedure. The proportion of sediment volume in size class *i* was used to estimate a probability:

$$p_i = (v_i/\Sigma v)/(\ln(D_i)-\ln(D_{i-1})) \quad (3)$$

where the sum over all size classes, Σv, gives total sediment volume and $(\ln(D_i)-\ln(D_{i-1}))$ gives the width of the ith class. A cubic spline was fit to these values to estimate a probability density function over the range of grain sizes. The spline was constrained so that integrated value over a size class equals the value given by Eqn. 3. The spline was then integrated over smaller increments to provide a larger number of grain-size classes for numerical integration of Eqn. 2.

For a channel segment, sediment flows in via fluvial transport from the upstream segment and erosion from adjacent hillslopes. Changes in the grain size distribution and losses to wash load (size-class 1, Table F-1) by abrasion are estimated through integration of Eqn. 2 over the length of the segment. This gives a total volume (or weight) by size class, for each segment.

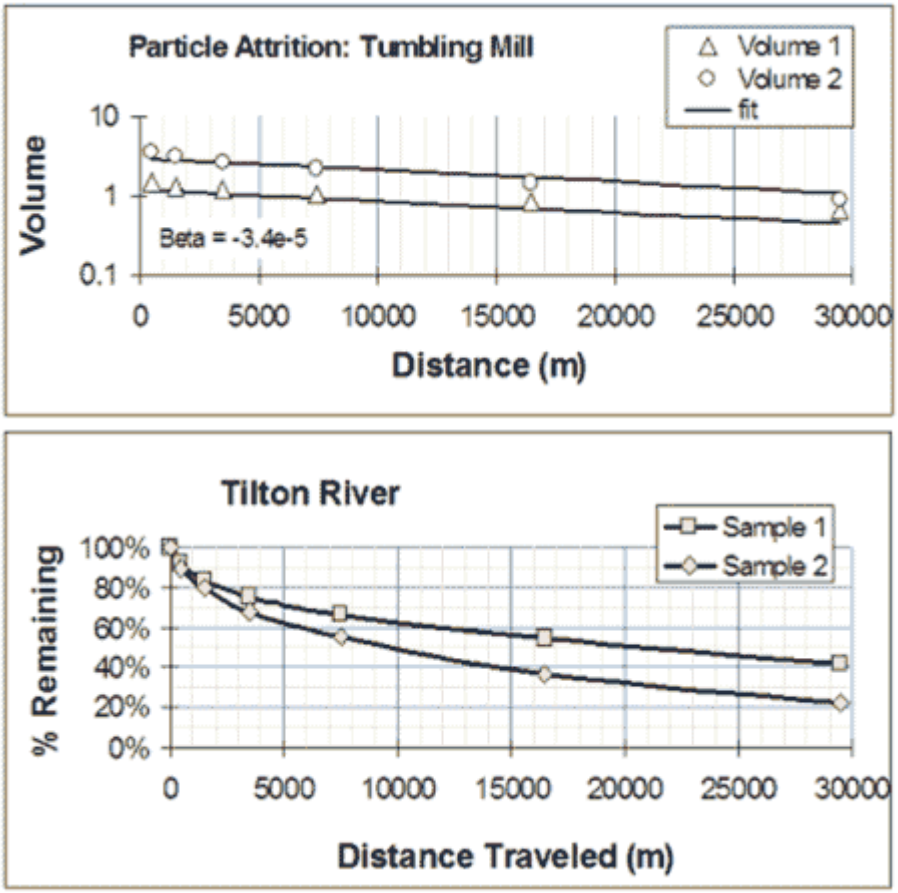

Figure F-1. Results of tumbling mill experiments for colluvium from the Tilton River basin (Earth Systems Institute, unpublished data).

Flood discharge

We use the estimated 2.3-year recurrence-interval flood discharge ($Q_{2.3}$) as an indicator of the channel-forming and bank-full flow (Wolman and Miller 1960, Whiting et al. 1999). The $Q_{2.3}$ was used rather than the $Q_{1.5}$ or Q_2 because cross-section measurements in the watershed indicated that effective discharge ranged from $Q_{1.5}$-Q_5 with $Q_{2.3}$ discharge the median. The $Q_{2.3}$ regression equations described for Sediment and Runoff (Appendix E) are a power function of drainage area:

$Q_{2.3} = 0.895317A^{0.925}$ (from gages above Merwin reservoir)

$Q_{2.3} = 0.967492A^{0.9132}$ (for the upper East Fork Lewis River)

Here $Q_{2.3}$ is in m^3/sec and drainage area A is in km^2.

These estimates are altered by land use in the watershed. Timber harvest or conversion of land from forest to agriculture, roads, or urban areas results in a proportional increase in $Q_{2.3}$, based on models described in Appendix E on sediment and runoff modeling. The proportional increase is calculated individually for each drainage wing, and then cumulatively summed over all upstream drainage wings to calculate land-use modifications to $Q_{2.3}$ for each segment.

Proportional increases in $Q_{2.3}$ for timber harvest and agriculture use are listed in Table F-1. Increases associated with agriculture vary with soil type, of which four broad types are delineated in the basin (described in Appendix A and Appendix E).

Table F-1. Increases in the estimated 2.3-year recurrence-interval flood discharge ($Q_{2.3}$) by land use and soil type

Land Use	Proportional increase in $Q_{2.3}$
Timber Harvest	0.08
Agriculture:	
Soil type 1	0.36
Soil type 2	0.12
Soil type 3	1.35
Soil type 4	0

The proportional increase in $Q_{2.3}$ associated with agriculture is calculated as $m_{ag} = \Sigma P_i m_i$, where P_i is the proportion of the area in agriculture in soil type i, m_i is the coefficient specified in Table F-1, and i varies from 1 to 4 (note that $\Sigma P_i = 1$).

Increases associated with roads are based on road density: if road density (ρ_{road}) exceeds 0.0012 m/m^2, $Q_{2.3}$ increases by 20%: $m_{road} = 0.0$, if $\rho_{road} \leq 0.0012$; $m_{road} = 0.2$, if $\rho_{road} > 0.0012$.

Increases associated with urban areas are calculated as $m_{urban} = P_{urban}*3.0 + 0.93$. Here P_{urban} is the proportion of area in urban cover types and m_{urban} is the proportional increase by which to modify $Q_{2.3}$. This equation gives a value less than one for values P_{urban} less than 0.023, in which case m_{urban} is set to one.

For each drainage wing, a modifier (DW_{mod}) for $Q_{2.3}$ is calculated as:

$$DW_{mod} = P_{Forest}*m_{forest} + P_{Ag}*m_{ag} + P_{urban}*m_{urban} + m_{road},$$

where P_{Forest} is the proportion of area in forest (and harvest) land cover, P_{ag} is the proportion of area in agriculture, and P_{urban} is the proportion of area in urban areas. Note that P_{Forest}, P_{ag}, and P_{urban} sum to one.

To estimate the increase in $Q_{2.3}$ for a segment, we use an area-weighted sum over all upstream drainage wings:

$$Q_{2.3} = Q_{2.3Base}\left(\frac{\sum\left(DW_{\mathrm{mod}(i)}A_{DW(i)}\right)}{\sum A_{DW(i)}}\right) \quad (4)$$

Here $Q_{2.3Base}$ is the baseline (unadjusted) discharge, $A_{DW(i)}$ is the area of the ith upstream drainage wing, and $DW_{mod(i)}$ is the modifier for the ith upstream drainage wing.

Bed Texture

Channel sediment texture is important for at least two reasons: 1) fry survival is affected by the proportion of fine sediment in the bed (Bjornn and Reiser 1991), and 2) the extent and depth of channel scour correlates with bedload transport rates, which are reflected in bed-sediment texture (Dietrich et al. 1989, Montgomery et al. 1996, Haschenburger 1999); increased transport rates correspond to finer surface grain sizes.

A simple empirical approach was used to characterize channel-bed sediments. First, we identified the physical factors that might affect sediment supply, transport, and deposition (restricted to those factors that can be quantified with available data). Then, we sought correlations between these factors and the bed textures (e.g., percentage of fine sediment) reported in available channel surveys.

Fine sediment is here defined as that large enough to be carried as bed load, but small enough to fill interstices of larger clasts and thereby impede water flow through the channel bed or hinder fry emergence. For the size classes listed in Table F-1, class 1 (< 0.25mm) is considered small enough to travel as wash load during high flows and classes 2-6 (> 0.25) are considered the bed load, with classes 2-3 (0.25 – 1.0mm) comprising the "fines" portion of the bed load.

Two sets of geo-referenced channel-survey data were used as general indicators of bed texture and abundance of fine sediments in channel substrates. One provided reach-averaged information for 16,133 m of channel over 12 reaches (HabRate Surveys conducted during field verification for this project, Table F-1). Two sets of these reaches were adjacent, so the survey provided information from 10 sites in the Lewis watershed. The other data were for a continuous habitat survey along 27,782 m of Cedar Creek (Jennifer Stone, USFWS, personal communication), a tributary to the North Fork below Merwin Dam used heavily by spawning steelhead. Data from both sources were aggregated to average values over reaches corresponding to the SHIAPP segments. Both surveys contained estimates of % fines (sand), % gravel, % cobbles, and % boulders for channel bed surfaces. The Cedar Creek surveys also included % bedrock. For the Cedar Creek dataset, Wolman pebble counts were summarized into percent substrate classes for each reach. Percent fines were calculated as the percent of total substrate measurements <6mm. For the HabRate dataset, % fines were assessed visually as the proportion of the substrate that was silt and organic matter, rather than from substrate size measurements.

A variety of field studies point to numerous factors that affect bed texture and % fines (Lisle 1989, Montgomery and Buffington 1997). The resolution and types of data available for characterizing channel attributes limit us, however, to a fairly small subset of these factors. The erosion models provide an indication of the locations and relative average rates of sediment inputs to the channel system; topographic information that can be inferred from the 10-m DEM provides an indication of gross channel morphology in terms of channel size, gradient, and valley confinement.

Sediment inputs, upstream sediment yield, and the 2.3-year-recurrence-interval flood discharge were estimated as described in Appendix E. Estimates of channel gradient, drainage area, and valley width were obtained with the NetStream program set (Miller 2003). Channel widths were provided from a separate calibrated model. While there was a regression equation of mean bank-full depth to drainage area based on channel geometry at Lewis basin gaging stations, we were interested in a depth estimate that responded to other attributes as well. Discharge through a cross section is

$$Q = WHU \qquad (5)$$

where

W is channel width

H is mean channel depth (cross-section area divided by width)

U is mean flow velocity through the cross section.

Mean flow velocity can be estimated with Manning's equation:

$$U = \frac{S^{1/2} R^{2/3}}{n} \qquad (6)$$

where

S is channel gradient

R is the hydraulic radius (cross section area divided by wetted perimeter: ~WH/(W+2H)), equal approximately to mean channel depth H

n is Manning's roughness coefficient.

Using the 2.3-year recurrence-interval discharge ($Q_{2.3}$) and an estimate of channel roughness, we can solve Eqn. 5 for mean flow depth H. In general, channel roughness is found to vary systematically with other channel attributes. Small, steep, coarse-bedded channels tend to have high roughness coefficients; large, low-gradient, fine-bedded channels tend to have low roughness coefficients. An empirical equation for mountain rivers that relates Manning's n to channel gradient and hydraulic radius was used (Jarrett 1984, Wohl 2000):

$$n = 0.32\, S^{0.38}\, R^{-0.16} \qquad (7)$$

Eqns. 5, 6, and 7 give H as

$$H = \frac{Q_{2.33}}{WU} = \frac{Q_{2.33}(0.32 S^{0.38} R^{-0.16})}{W S^{1/2} R^{2/3}} \qquad (8)$$

Eqn. 8 can be solved iteratively (R is also a function of H) to provide a flow-depth estimate for every segment. This estimate is a function of channel width, channel gradient, and discharge (which is itself a function of drainage area and upstream land use).

If we assume equilibrium between estimated sediment inputs and fluvial transport rates, we can use a simple bed-load transport model to make further inferences about bed texture. Empirical measures of bed-load transport are commonly characterized in the form

$$q_s = a(\tau - \tau_c)^b \quad (9)$$

where

q_s is bed-load transport rate per unit channel width

τ is available shear stress at the channel bed

τ_c is the "critical" shear stress required to initiate transport

a and *b* are empirical coefficients

The Meyer-Peter and Müller equation, for example, gives a value for *a* of approximately $8\rho/(g(\rho-\rho_s)\rho^{3/2})$, where ρ is water density, ρ_s is sediment density, and g is gravitational acceleration, and a value for *b* of 3/2. The critical shear stress is a function of bed texture, and is estimated from the empirical Shields stress:

$$\tau^* = \frac{\tau_c}{g(\rho - \rho_s)D} \quad (10)$$

where D is a characteristic grain size for channel-bed sediments. From 10,

$$\tau_c = \tau^* g (\rho - \rho_s) D. \quad (11)$$

Equations 10 and 11 give

$$D = \frac{\tau - \left(\frac{q_s}{a}\right)^{1/b}}{g(\rho - \rho_s)\tau^*} \quad (12)$$

Table F-1. Reach-averaged results of HabRate surveys conducted in the Lewis River watershed.

Stream	Length (m)	Width (m)	Area (m2)	Slope (%)	Depth (m)	% Silt/Org	% Sand	% Gravel	% Cobble	% Boulder	% Bedrock
Clear Creek	1397.0	8.82	242.5	1.17	0.79	8.28	22.21	35.33	32.22	2.05	0.00
Copper Creek	2031.4	7.37	208.9	4.21	0.62	0.35	3.41	19.47	25.36	24.45	27.05
EF Lewis River	1363.2	19.07	2104.6	0.85	0.78	1.93	9.93	19.93	42.73	25.47	0.00
Johnson Creek 1	848.2	4.09	88.4	7.37	0.41	2.40	16.38	32.20	21.03	5.28	22.63
Johnson Creek 2	908.7	4.24	72.5	1.89	0.29	3.3	15.77	34.35	33.35	12.77	0.44
Mason Creek	1318.63	4.36	233.9	0.48	0.6	40.21	8.46	33.68	17.11	0.46	0.00
Miller Creek	1086.5	2.67	31.6	10.94	0.29	2.55	12.58	13.94	25.25	44.58	1.07
NF Lewis River 1	1547.4	19.19	1826.6	0.87	1.42	0.00	9.60	15.70	26.45	27.40	20.80
NF Lewis River 2	2606.8	22.68	3169.2	0.50	0.83	0.00	16.92	25.00	34.72	21.20	1.72
Pine Creek	3399.7	8.37	376.5	4.10	0.58	0.05	19.24	20.79	28.04	31.73	0.13
Rock Creek	1413.87	10.39	513.2	0.86	0.58	3.44	9.94	33.59	29.53	10.84	12.78
Siouxon Creek	1295.20	15.89	800.71	3.01	0.96	0.85	6.19	15.52	19.78	38.59	18.81

For gravel-bed channels, τ^* is nearly constant in the range of 0.03 to 0.045 (Buffington and Montgomery 1997). Using a value for τ^* of 0.03 (Buffington and Montgomery 1999a), values for *a* and *b* from the Meyer-Peter and Müller equation, and the depth-slope product ($\tau = \rho gSH$) for shear stress, Eqn. 12 provides an estimate of the characteristic grain size associated with a transport rate q_s.

If we assume that most sediment transport occurs during bankfull discharge, approximated in the Lewis basin with $Q_{2.3}$, transport rate q_s is approximated as

$$q_s \approx Q_S / (W*T)$$

where

Q_S is total sediment input from upstream, estimated as mean annual sediment yield

W is channel width

T is the duration of bankfull flow, estimated as 2.1 days, the average for Lewis River basin streams.

The assumption of equilibrium between sediment inputs and outputs, so that q_s can be estimated from mean annual sediment yield, is a purely conceptual construct. Sediment production and transport is highly stochastic (e.g., Benda and Dunne 1997) and transit times through valley segments can vary dramatically (Reid and Dunne 1996). Likewise, sediment transport may occur over a range of discharges. Indeed, with these assumptions, Eqn. 12 specifies a negative characteristic grain size for many segments. Nevertheless, this calculation serves a useful purpose. It provides a spatially distributed estimate of potential supply relative to potential transport. Small values of D correspond to segments where supply is large relative to transport potential (transport-limited, response reaches); large values correspond to segments where supply is low relative to transport potential (supply-limited, transport reaches). The value of D obtained with Eqn. 12 responds both to changes in $Q_{2.3}$, via changes in the estimated flow depth used to calculate shear stress τ, and to changes in estimated sediment supply. Increased discharge results in an increase in D; increased supply causes a decrease in D.

We can use the same approach to evaluate the potential effect of local sediment supply on bed texture. Rather than sediment yield for the entire upstream watershed, q_s can be based on some measure of local sediment input. I defined a local measure of sediment flux using a distance-weighted sum of upstream sediment inputs, with a weighting that decreases exonentially with distance upstream:

$$Q_{Slocal} = \Sigma(Q_{Si}\, e^{-\alpha x_i}) \quad (13)$$

Where

Q_{Slocal} is a measure to characterize total sediment flux through the channel from local upstream sources

Q_{Si} is sediment input from the ith upstream drainage wing

x_i is distance to the ith upstream segment.

The coefficient α is set to cause the weighting term to decrease by one half over a specified distance $x_{1/2}$, i.e., $\alpha = \ln(0.5)/x_{1/2}$. We found a value of $x_{1/2}$ = 500m worked well for correlating observed channel textures to local sediment inputs. Together, these methods provide channel attributes such as proportion of fines (Table F-2).

Table F-2. Estimated channel attributes

Attribute	Source
Gradient (S)	DEM (NetStream, using intersection of channel arcs and 40-ft contour lines)
2.3-yr recurrence interval flood ($Q_{2.3}$)	Function of drainage area, modified by watershed land use
Mean annual upstream bed load (Q_S)	Erosion models, abrasion
Stream power (Q_S)	Product of $Q_{2.3}$ and gradient S
Local sediment inputs (Q_{Slocal})	Erosion models, distance upstream
Proportion of bed load sediment in fine size class (P_F for total watershed yield and P_{Flocal} for locally derived sediment)	Based on grain size distribution for incoming fluvial sediment and local upstream drainage wings
Channel width (W)	Calibrated function of drainage area, mean annual precipitation, and channel gradient
Mean bank-full depth (H)	Function of $Q_{2.3}$, channel gradient, and channel width
Valley width	DEM (NetStream)
Maximum reach-averaged shear stress (τ)	Calculated from gradient and flow depth (ρgHS)
Valley-width index (VWI)	Ratio of valley width to channel width
dS/dx, dW/dx, dVWI/dx	Longitudinal changes in channel gradient, channel width, and valley width
Characteristic bed grain size based on transport rate (D)	Function of sediment supply and maximum reach-averaged shear stress

Proportion Fine Sediment

Correlations between channel attributes (Table F-2) and the % fines reported in the HabRate and Cedar Creek surveys (noting that many of the attributes are themselves correlated) were evaluated. The HabRate data exhibited relationships with three attributes (Figure F-2), listed in order of decreasing importance:

- P_{Flocal}, the proportion of local sediment inputs (using the distance-weighted sum defined above) in fine size classes (classes 2 and 3 in Table F-1, 0.25-1.0mm),
- VWI, the valley width index, and
- Q_S, stream power.

No significant correlations were found for any of the other variables. These observations led us to infer that the % fines reported in the HabRate survey depends primarily on the grain-size distribution of local upstream sediment inputs (as represented by the erosion

models, which respond to soil types, hillslope gradients, and land cover), modulated by channel characteristics represented with the valley-width index and estimated stream power:

$$\%Fines = a_1 P_{Flocal}^{b1} (1 + (a_2 + c_2 VWI^{b2}) + (a_3 + c_3 QS^{b3})) \qquad (14)$$

$$= a_1' P_{Flocal}^{b1} (1 + a2' VWI^{b2} + a_3' QS^{b3})$$

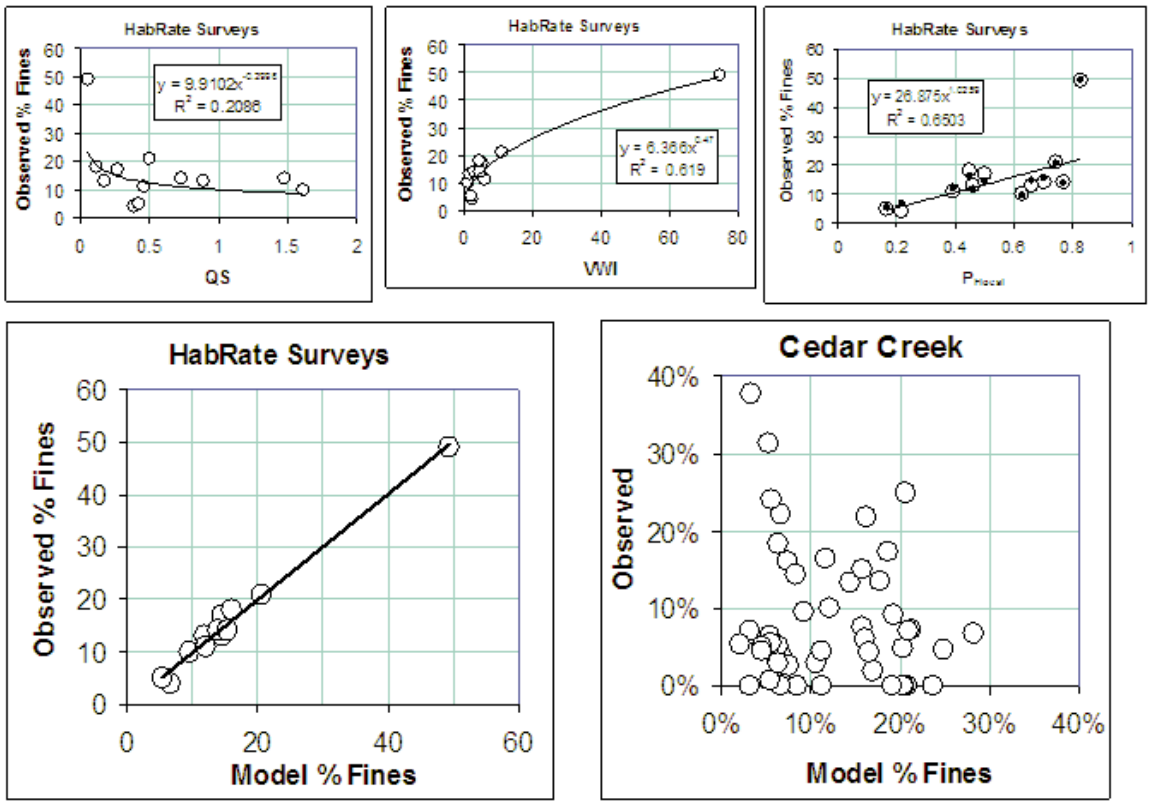

Figure F-2. Upper graphs show relationships between stream power (QS), valley-width index (VWI), and the proportion of local sediment inputs in fine (0.25-1.0mm) size classes (PFlocal). The black lines show power-function regressions to the data. The small black dots in the right-most graph show adjustments in estimated values when effects of stream power and channel confinement (via VWI) are included in the model. Lower graphs show correlation between modeled and observed values. The model was calibrated to the HabRate surveys. The Cedar Creek values showed no relationship to any geomorphic attributes (Table F-2) and the HabRate model bears no relationship to observed values at Cedar Creek.

Coefficients were obtained using the "Solver" module in Microsoft Excel to minimize RMS (root-mean square) differences between the %Fines calculated with Eqn. 14 and reported values. Power functions are used so that the influence of large values can be reduced (e.g., the influence of valley width on channel confinement changes little beyond a valley width index of 10 or so, as indicated by the small exponent given by value b2 in Table F-3). Although this model fits the observations well, it is based on few samples, has half as many parameters as data points, and is heavily influenced by one large data value. The conceptual model for Eqn. 14 and the relative magnitude of the fit parameters do correspond to physical expectations, but our ability to predict observations elsewhere in the basin may be very limited. While analyses of significance for these coefficients were not done, we can evaluate the predictive ability of the model using the HabRate and

Cedar Creek data. As shown in Figure F-2, the HabRate model has a positive relationship but the Cedar Creek model has no relationship to the observed %sand.

This failure is not necessarily an indication that the model has no worth; it may simply be a consequence of the great potential heterogeneity exhibited by processes of sediment supply and transport (Benda et al. 1998) as reflected in resulting substrate texture. It might also indicate differences in survey techniques. The Cedar Creek survey, although of longer total length than the HabRate surveys, is limited to a single channel, whereas the HabRate data reflect ten different locations in the watershed. These ten sites may provide a better indication of channel response than obtained with data from a single channel. Moreover, the value representing % fines in the Cedar Creek dataset included sediment particles of up to 6mm, which is likely larger than that considered to be "silt" in the HabRate dataset. In the absence of additional data, Eqn. 14 provides a model for estimating the proportion of fines expected in channel-bed sediments. It is responsive both to changes in local sediment supply and to changes in discharge, which serves the need for simulating relative effects of different land use scenarios in the basin.

Table F-3. % Fines model coefficients (pre-test model)

Coefficient	Value
a_1'	0.231
b1	0.610
a_2'	47.600
b2	0.292
a3'	5.200
b3	-0.928

Test and Revision of the % Fines Model

Initial scenarios to examine the effects of road decommissioning resulted in increased percent fines in some channel reaches. The model for percent fines is based on correlations with three independent variables: the proportion of locally derived sediment in fine size classes, channel width to valley width (valley width index), and an estimate of stream power (the product of the modeled 2.33-year-recurrence interval flood discharge and DEM-estimated channel gradient). Roads enter the sediment models in two ways: there is erosion from road surfaces and road density enters calculations of mass wasting. Removing road segments therefore reduces both surface erosion and mass wasting sediment sources, which each contribute different sediment grain-size distributions.

For most channel segments, surface erosion (excluding roads) contributes the majority of all sediment, and this sediment is predominately fine grained. Coarse-grained sediment comes primarily from mass wasting. Eliminating the mass-wasting sediment associated with roads reduces the total sediment input, but by eliminating a source of coarse sediment, can increase the proportion of the sediment supplied that is in fine size classes. Since this proportion is the factor that influences the predicted percentage of fines in the bed, and not the total amount of sediment supplied, the result is an increase in the predicted percentage of fines in the channel bed.

Two potential problems with the modeling methods were identified. First, surface erosion, particularly from roads, occurs with every rainstorm, whereas landsliding is

considerably less frequent. Within any single drainage wing, most years probably have no landslides. Our models utilize estimated long-term mean annual sediment inputs, but what one finds in the channel bed might depend more on what has occurred in the last few years. We may capture average conditions better using only the chronic sediment sources – surface erosion and roads – and not using mass wasting inputs for predicting the percentage of fines in the channel bed. Second, surface erosion of road surfaces predominately produces sediment that is fine enough to be suspended by overland flow over the road, generally less than 1.0 mm. We have been using the grain-size distribution associated with surface erosion, which although primarily of finer size classes, includes a proportion of coarse sediment.

To address the first point, mass-wasting sediment was excluded from the analysis. The model was recalibrated using only sediment from surface and road-erosion sources. The resulting coefficients were very similar and the goodness of fit unchanged. However, because surface erosion and road erosion both contribute the same size-class distribution within our models, this change would not result in any reduction in the percentage of fine sediment in channel beds associated with road removal

To address the second point, we altered the grain-size distribution for sediment derived from roads to exclude size classes greater than 1.0 mm. The incoming sediment was divided between the < 0.25, 0.25-0.5, and 0.5-1.0 mm size classes in the proportions specified for these three classes for surface erosion. This time, recalibration of the model resulted in a very slightly better fit.

These changes give us a model with coefficients that fit our limited observations just as well as the previous set, but that should result in a reduction in predicted percent fines in the channel bed when roads are decommissioned (Table F-4). This results because 1) roads now contribute only fine sediment, and 2) changes in mass wasting associated with removing (or adding) roads do not affect the predicted percentage of fines in the bed.

The revised model (Equation 14):

$$\%Fines = a_1 P_{Flocal}^{b1} (1 + (a_2 + c_2 VWI^{b2}) + (a_3 + c_3 QS^{b3}))$$

$$= a_1' P_{Flocal}^{b1} (1 + a2' VWI^{b2} + a_3' QS^{b3})$$

Table F-4. Updated % fines model coefficients:

Coefficient	Value
a_1'	0.207
b1	0.860
a_2'	54.093
b2	0.342
a3'	4.955
b3	-0.493

Proportion Coarse Sediment

Bed-surface texture can provide an indication of bed load transport rate, with finer textures indicative of larger transport (Dietrich et al. 1989, Buffington and Montgomery 1999). Texture is also influenced by local inputs (e.g., the boulders found in debris-flow deposition zones). Transport rate and local sediment inputs are important determinants

for many channel attributes (Church 2002), including depth of scour. As described above, we can use modeled sediment inputs to the channel system to estimate transport rates (assuming equilibrium with upstream sediment yield) and local sediment inputs. We can use the sediment models, together with other estimated channel attributes that affect transport capacity (channel gradient, channel width, and flow depth), to predict variations in bed texture, in terms of a characteristic grain size, throughout the channel network (Eqn. 12). This hypothesis can be tested against the HabRate and Cedar Creek survey data.

The D value was calculated for all segments using both total sediment yield and local sediment inputs, as described previously (Eqn. 12). Using the sum of % cobbles and % boulders (and % bedrock for Cedar Creek) as an indicator of bed texture (i.e., % coarse), comparison with surveyed values are shown in Figure F-3. Using total sediment yield to estimate transport rate in Eqn. 12 provides no relationship between the calculated grain size D and observed bed textures. However, characteristic grain size based on local sediment supply correlates with observed textures in both cases. There is a large degree of scatter, but a clear trend exists. For the HabRate survey, correlations are also found with the proportion of locally supplied sediment in size classes 4 and 5 (>4.8mm, Table F-1) and with valley width index. Such correlations are evident, but much weaker for the Cedar Creek data.

These results suggest that estimates of shear stress and local sediment supply (Eqn. 12) provide a useful indicator of bed texture. This model is responsive to changes in flow, which by altering estimated flow depth (and associated shear stress), indicates a coarsening of bed texture with increased discharge, and changes in local sediment supply, with increased supply indicating a fining of bed texture. Although this model ignores other types of channel response, such as changes in width or gradient, it provides an indication of the magnitude of response that may be associated with changes in the watershed that affect rates of runoff and erosion.

Using the HabRate data, we can incorporate predicted characteristic grain size (Eqn. 12), the proportion of locally supplied sediment in the fine size fraction (0.25 – 4.8mm), and the valley width index into a calibrated model to predict the coarse fraction of channel bed sediments. Following the reasoning for Eqn. 14, we define a model:

$$\text{Coarse_Fraction} = a_1 D^b (1 + a_2 P_{Flocal} + a_3 VWI) \qquad (15)$$

Here P_{Flocal} is the proportion of local sediment inputs ("local" as defined previously, using an exponential weighting with distance) in size classes 1-3 (0.25-4.8 mm, Table F-1). As before, coefficients are estimated using Excel Solver to minimize the RMS error. Residuals indicated no nonlinear dependence on P_{Flocal} or VWI (with VWI cut off at a value of 10, i.e., MIN(VWI,10)), so no exponents were used with these variables. Coefficient values are supplied in Table F-5.

Table F-5. Coarse-fraction coefficient values.

Coefficient	Value
a_1	108.800
b	0.143
a_2	-0.192
a_3	-0.0524

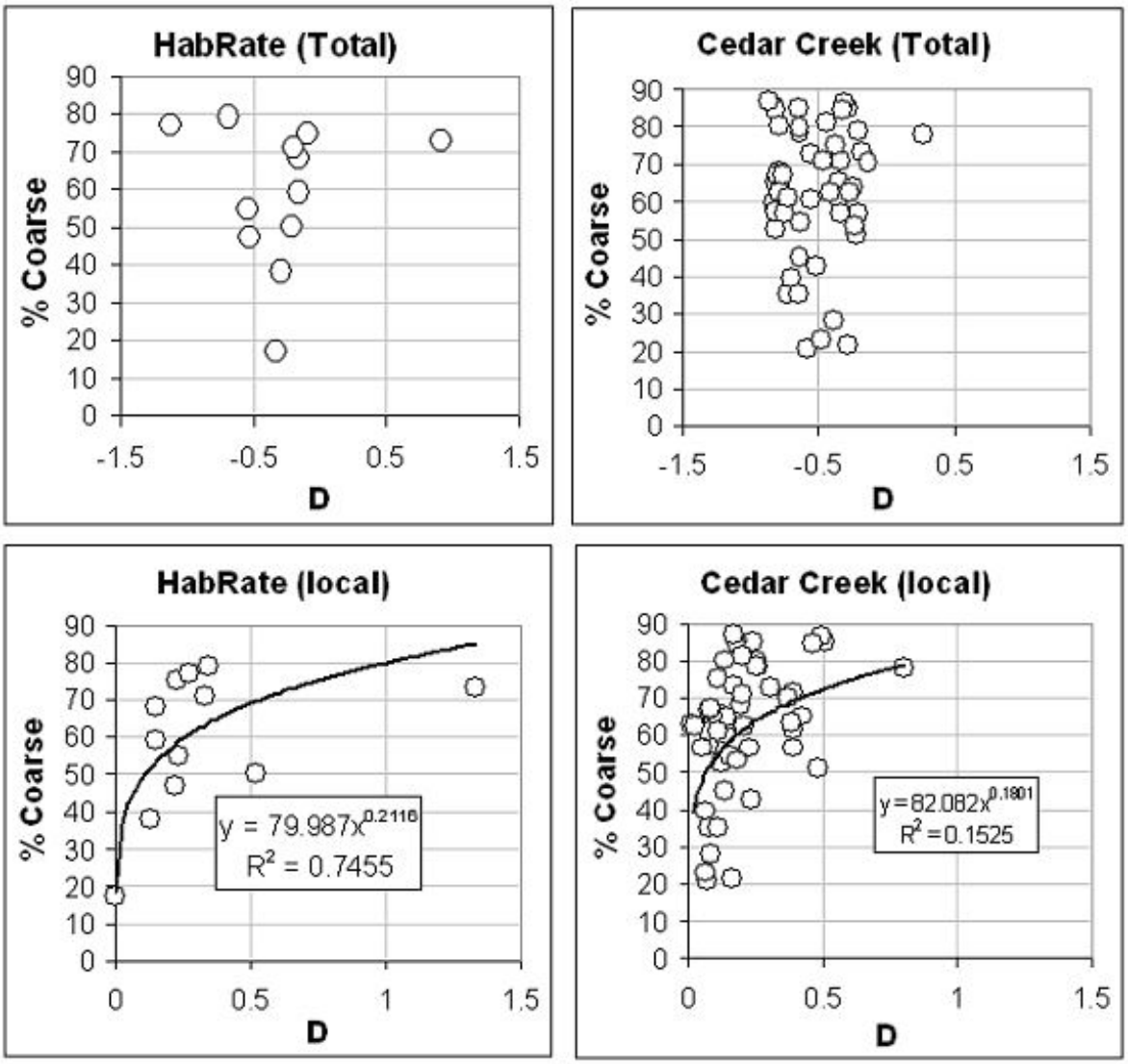

Figure F-3: Characteristic bed grain size based on bed load transport rate (Eqn. 12). Use of total watershed yield shows no relationship (upper graphs); use of local sediment inputs to estimate transport rate shows consistent trends for both data sets (lower graphs).

Bed Scour

Over reach-averaged length scales (tens to hundreds of meters), the depth, frequency, and spatial extent of scour is observed (or expected) to vary with numerous factors, including bedload transport rates and associated shear stress (channel depth and gradient) and bed texture (Montgomery et al. 1996, Haschenburger 1998), channel confinement (Schuett-Hames et al. 1994), flood discharge (Haschenburger 1998), and the amount of stable large woody debris. These factors are themselves inter-related.

The channel attributes and models for characteristic grain size described above incorporate the first three of these factors, bed load transport rate, channel confinement, and flood discharge. We therefore have the ingredients for a model of relative bed scour.

Following is a list of factors available to us that we might include in a model of scour:

- Flood discharge $Q_{2.3}$ (increased discharge causes increase in mean scour depth)
- Shear stress $\tau \approx \rho hHS$ (increased shear stress causes increase in mean scour depth)
- Characteristic grain size D (function of shear stress and sediment supply, smaller D corresponds to increased mean scour depth)
- Fine fraction in bed surface (related to D, higher proportion fines corresponds to increased mean scour depth)
- Valley width index (less confined channels tend to exhibit greater scour)

All factors are inter-related and exhibit non-linear relationships to scour. A simple model using some combination of these that might be related to scour can be hypothesized, but we currently lack data to evaluate or calibrate such a model. A combination of the above factors is given by an index

$$I_S = QS/WD_{pred} \qquad (16)$$

where D_{pred} is the characteristic grain size predicted by regressing the coarse-fraction model (Eqn. 15) against the D value from Eqn. 12. D_{pred} incorporates all the factors in Eqn. 15: local bedload supply, the fine fraction of the local supply, and channel confinement (via the valley-width index). D_{pred} relates to bed texture, in that larger D_{pred} values are associated with coarser beds, but its relationship to any quantified aspect of the grain size distribution is unknown, and perhaps unwarranted. Thus I_S has all the components required for an index of scour potential, but with no quantitative relationship established to actual scour.

To establish a relative relationship, we can use the distribution of calculated I_S values as a guide. Figure F-4 shows a cumulative distribution of I_S for channels of drainage area greater than one square kilometer and DEM-estimated gradients of less than 7% (approximating the fish-bearing portion of the network). We can set thresholds to define "high," "moderate," and "low" ranges. For example, for the current scenario, 50% of the fish-bearing network is low, 30% moderate, and 20% high. The value of such arbitrarily defined thresholds is in comparing the proportion of the channel network falling within these classes under different scenarios. Additionally, because a value is defined for each segment, the locations experiencing changes in scour potential between different scenarios can be identified.

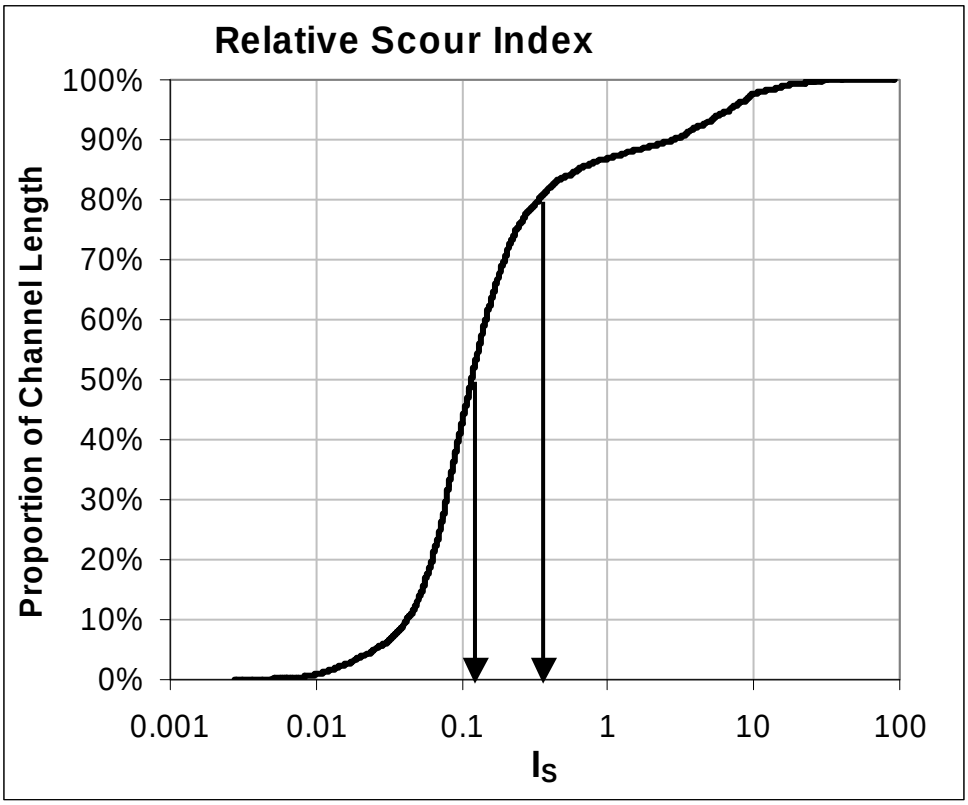

Figure F-4. Cumulative distribution of "scour index" (I_S, Eqn. 16) over low-gradient (< 7%, potentially fish-bearing) channels. This distribution can be used to define thresholds to compare scour potential between different scenarios. In this case, for example, 50% of all values fall to the left of the left-most arrow and 20% of all values fall to the right of the right-most arrow. Using the corresponding I_S values, the proportions will differ with different scenarios: if the proportion falling to the right increases, scour potential in the basin has increased.

References

Benda, L. E., and T. Dunne. 1997. Stochastic forcing of sediment supply to channel networks from landsliding and debris flow. Water Resources Research 33:2849-2863.

Benda, L. E., D. J. Miller, T. Dunne, G. H. Reeves, and J. K. Agee. 1998. Dynamic landscape systems. Pages 261-288 in R. J. Naiman and R. E. Bilby, editors. River Ecology and Management. Springer-Verlag, New York.

Bjornn, T. C., and D. W. Reiser. 1991. Habitat requirements of salmonids in streams. in W. R. Meehan, editor. Influences of Forest and Rangeland Management on Salmonid Fishes and Their Habitats. American Fisheries Society, Bethesda, Maryland.

Buffington, J. M., and D. R. Montgomery. 1997. A systematic analysis of eight decades of incipient motion studies, with special reference to gravel-bedded rivers. Water Resources Research 33:1993-2029.

Buffington, J. M., and D. R. Montgomery. 1999a. Effects of hydraulic roughness on surface textures of gravel-bed rivers. Water Resources Research 35:3507-3521.

Buffington, J. M., and D. R. Montgomery. 1999b. Effects of sediment supply on surface textures of gravel-bed rivers. Water Resources Research 35:3523-3530.

Church, M. 2002. Geomorphic thresholds in riverine landscapes. Freshwater Biology 47:541-557.

Dietrich, W. E., J. W. Kirchner, H. Ikeda, and F. Iseya. 1989. Sediment supply and the development of the coarse surface layer in gravel-bedded rivers. Nature 340:215-217.

ESRI. 1998. ESRI Shapefile technical description. ESRI White Paper.

Haschenburger, J. K. 1998. Channel scour and fill in coastal streams. Pages 109-117 in D. L. Hogan, P. J. Tschaplinski, and S. Chatwin, editors. Carnation Creek and Queen Charlotte Islands Fish/Forestry Workshop: Applying 20 years of Coastal Research to management Solutions: Land Management Handbook 41. B.C. Ministry of Forests, Victoria, B.C.

Haschenburger, J. K. 1999. A probability model of scour and fill depths in gravel-bed channels. Water Resources Research 35:2857-2869.

Jarrett, R. D. 1984. Hydraulics of high-gradient streams. Journal of Hydraulic Engineering 110:1519-1539.

Lisle, T. 1989. Sediment transport and resulting deposition in spawning gravels, North Coastal California. Water Resources Research 25:1303-1319.

Mikos, M. 1995. Fluvial abrasion: converting size reduction coefficients into weight reduction rates. Journal of Sedimentary Research A65:472-476.

Miller, D. J. 2002. Programs for DEM Analysis. Earth Systems Institute, Seattle, WA. , Available at: http://www.fsl.orst.edu/clams/.

Miller, D. J. 2003. Programs for DEM Analysis. in Landscape Dynamics and Forest Management, General Technical Report RMRS-GTR-101CD. USDA Forest Service, Rocky Mountain Research Station, Fort Collins, CO, USA.

Montgomery, D. R., and J. M. Buffington. 1997. Channel-reach morphology in mountain drainage basins. Geological Society of America Bulletin 106:596-611.

Montgomery, D. R., J. M. Buffington, N. P. Peterson, D. Schuett-Hames, and T. P. Quinn. 1996. Stream-bed scour, egg burial depths, and the influence of salmonid spawning on bed surface mobility and embryo survival. Canadian Journal of Fisheries and Aquatic Science 53:1061-1070.

Parker, G. 1991. Selective sorting and abrasion of river gravel. I: Theory. Journal of Hydraulic Engineering 117:131-149.

Reid, L. M., and T. Dunne. 1996. Rapid Construction of Sediment Budgets for Drainage Basins. Catena-Verlag, Cremlingen, Germany.

Schuett-Hames, D., N. P. Peterson, and T. P. Quinn. 1994. Patterns of scour and fill in a low-gradient alluvial channel. Part C, Chapter 1. Pages 42-55 in T. P. Quinn and N. P. Peterson, editors. The Effect of Forest Practices on Fish Populations, Report TFW-F4-94-001. Washington Dept. of Natural Resources, Olympia.

Salmon and Steelhead Habitat Inventory and Assessment Program (SSHIAP). 2004. Unpublished spatial data on hydrology and stream conditions (1:24,000) for Watershed Inventory Area (WRIA) 27.

Steel, E. A., M. Sheer, P. Olson, A. Fullerton, J. Burke, D. Jensen, and L. Johnston. 2003. Habitat Analyses for the Lewis River Case Study: Interim Report. NW Fisheries Science Center, NOAA Fisheries, Seattle.

Whiting, P. J., J. F. Stamm, D. B. Moog, and R. L. Orndorff. 1999. Sediment-transporting flows in headwater streams. Geological Society of America Bulletin 111:450-466.

Wohl, E. 2000. Mountain Rivers. American Geophysical Union, Washington, D.C.

Wolman, M. G., and J. P. Miller. 1960. Magnitude and frequency of forces in geomorphic processes. Journal of Geology 68:54-74.